Nuclear Instruments and Methods in Physics Research A 780 (2015) 107–113

Contents lists available at ScienceDirect

Nuclear Instruments and Methods in Physics Research A

journal homepage: www.elsevier.com/locate/nima

An internal ALD-based high voltage divider and signal circuit for MCP-based photodetectors

Bernhard W. Adams [b], Andrey Elagin [a], Jeffrey W. Elam [b], Henry J. Frisch [a,*], Jean-Francois Genat [a,1], Joseph S. Gregar [b], Anil U. Mane [b], Michael J. Minot [c], Richard Northrop [a], Razib Obaid [a,2], Eric Oberla [a], Alexander Vostrikov [a], Matthew Wetstein [a]

[a] Enrico Fermi Institute, University of Chicago, United States
[b] Argonne National Laboratory, United States
[c] Minotech Engineering, Inc and Incom, Inc, United States

ARTICLE INFO

Article history:
Received 9 December 2014
Received in revised form
30 December 2014
Accepted 2 January 2015
Available online 23 January 2015

Keywords:
Photodetector
Micro-channel plates
High voltage
Large-area photodetectors
Picosecond time resolution
Vacuum tube

ABSTRACT

We describe a pin-less design for the high voltage (HV) resistive divider of the all-glass LAPPD™ 8 in.-square thin photodetector module. The divider, which distributes high voltage applied to the photocathode to the two micro-channel plates (MCPs) that constitute the amplification stage, is comprised of the two MCPs and three glass mechanical spacers, each of which is coated with a resistive layer using atomic layer deposition (ALD). The three glass grid spacers and the two MCPs form a continuous resistive path between cathode and anode, with the voltages across the MCPs and the spacers determined by the resistance of each. High voltage is applied on an external tab on the top glass window that connects to the photocathode through the metal seal. The DC ground is supplied by microstrips on the bottom glass plate that form the high-bandwidth anode. The microstrips exit the package through the glass-frit seal of the anode base-plate and the package sidewall. The divider is thus completely internal, with no HV pins penetrating the low-profile flat glass package. Measurements of the performance of the divider are presented for the 8 in.-square MCP and spacer package in a custom test fixture and for an assembled externally pumped LAPPD™ prototype with an aluminum photocathode.

1. Introduction

The LAPPD Collaboration [1] was formed to develop large-area photodetectors based on micro-channel plates [2] for precise time-of-flight measurements in large-scale detectors for High Energy Physics. In a number of applications the ability to detect the arrival of multiple photons in a large-area plane, each measured with a time resolution measured in pico-seconds ($1\ \text{ps} = 10^{-12}\ \text{s}$) and a space resolution measured in millimeters, enables a 3D pattern reconstruction using the 2D position of arrival of each photon and the transit time to determine the remaining orthogonal third component [3]. Additionally, a ps-level measurement of the time coordinate allows a qualitative change in the photodetector area needed to provide a given level of coverage for large diffuse sources such as the large water-Cherenkov or scintillation counters used in particle and nuclear physics, as the addition of the transit drift time of the photon transforms a 2-dimensional phase space into a much larger 3-dimensional space. Optical systems can take advantage of measuring both the position and the time of arrival to minimize expensive photocathode area while still preserving space resolution.[3]

The amplification in conventional discrete-dynode photomultipliers (PMTs) and microchannel-based photomultipliers (MCP–PMTs) is done by electron multiplication, with the electrons accelerated between collisions with a dynode (in a PMT) or the wall of a capillary channel (in an MCP–PMT) to provide energy for secondary electron emission. The multiplication is consequently exponential, and depends on the secondary-emission yield (SEY) of each collision and the number of collisions (equal to the number of dynodes in a PMT). The SEY in turn depends on the accelerating voltage between

* Corresponding author. Tel.: + 1 773 702 7479; fax: +1 773 702 1914.
E-mail address: frisch@hep.uchicago.edu (H.J. Frisch).
[1] Present address: Universités Pierre et Marie Curie, Paris, France.
[2] Present address: Physics Department, University of Connecticut, Storrs, CT 06269, USA.

[3] One can think of this as similar to rotations between transverse and longitudinal emittances in accelerators.

http://dx.doi.org/10.1016/j.nima.2015.01.034
0168-9002/

collisions, which in a PMT is typically set by a resistive voltage divider that supplies each dynode from a high voltage (HV) source at the input to the divider. The principle is the same in an MCP–PMT, but rather than a divider made of discrete resistive elements, the voltages between collisions are set by a DC current flowing through a resistive layer on the walls of the capillaries. In an MCP–PMT with the typical pair of capillary plates as an amplification section, voltage is usually applied to the top and bottom of each plate by deposition of a conducting electrode surface.

LAPPD™ (large area picosecond photodetector) is an MCP-based photodetector, capable of imaging at high spatial and temporal resolution, in an ultra-high vacuum (UHV) hermetic package with an active area of 400 cm^2. The modular detector design is based on a hermetic all-glass vacuum tube package consisting of a thin window on which a bialkali photocathode has been deposited, two 8 in.-square micro-channel plates (MCP), and an anode implemented as high-bandwidth RF silver micro-striplines [4]. Amplification is provided by a pair of micro-channel glass substrates [5] coated by atomic layer deposition (ALD) [6], with typical gains of more than 10^7.

The HV distribution for the LAPPD™ can be implemented in a number of ways, depending on the application and possibly also on parameters of the production process. In the design described here, the HV distribution and the high frequency signal path are both integral parts of an economical mechanical structure. The hermetic package has only 8 parts, all made of commonly available sheet glass. The only additional element is a simple getter assembly formed from a strip of getter material and glass bead supports that is situated around the circumference of the channel plate stack assembly. An attractive feature for robustness and fabrication yield is that there are no pins penetrating the package; both the HV and the anode signals are brought in through metal layers deposited on the glass prior to assembly. The planar anode signal plane has an analog bandwidth of 1.6 GHz (3 db loss) [4] in this implementation.

The organization of the paper is as follows. Section 2 describes the resistive HV distribution chain, with the resistive elements and DC current path described in Sections 2.1 and 2.2, respectively. The high-speed (radio-frequency, RF) signal circuit, which is electrically and mechanically integrated with the HV circuit, is discussed in Section 2.3 for the usual configuration with the anode pattern on the inside surface of the vacuum volume (Section 2.3.1), and a capacitively coupled configuration with pads or microstrips on the outside surface (Section 2.3.2). The integration of the HV divider into the LAPPD™ hermetic package is described in Section 3, where the physical dimensions, ALD coating parameters, and electrical values are also summarized.

Measurements of the performance of the HV divider are presented in Section 4. A summary of the test facilities for the HV chain is given in Section 4.1. Section 4.1.1 describes a custom test facility, the spacer station (ISS), used to make DC measurements of current and voltage. A second test facility, the 'demountable tile', consisting of an LAPPD™ glass-body tile mechanical assembly, but with an O-ring window seal and a permanent connection to a vacuum pump rather than being a hermetically sealed tube, is used to make measurements of fast pulses, including time and space resolutions, as described in Section 4.1.2. Measurements of *I–V* curves and the dependence of the divider resistance on temperature, pressure, and time are presented in Sections 4.2–4.5. The paper concludes with a summary in Section 5.

2. The HV resistive distribution chain

The hermetic package, made of readily available borosilicate glass [7], consists of a top window, sidewall, and anode bottom plate. The sidewall is hermetically sealed to the anode plate with glass frit to form a robust base unit. The top window is sealed with indium to the base in vacuum after the photocathode is deposited. HV is applied outside the vacuum volume on a window tab that makes contact with the metalized border of the window and the photocathode. Resistive grid spacers coated by ALD support the pressure on the top window and bottom anode plate. The three spacers and the two MCP plates, together with the (DC) grounded anode plane, form the resistive HV divider that determines the voltages across the MCPs and the three gaps. The silver anode strips [8] extend beyond the sidewall bottom seal to complete the electrical circuits for both signals and DC current. Atmospheric pressure transmitted through the top window and bottom anode plane compresses the 'stack' of grid spacers and microchannel plates into a rigid thin package.

A diagram of the layers of the HV divider is shown in Fig. 1.

2.1. Resistive components

Amplification in the tile is provided by a pair of microchannel-plates with 20 μm-diameter pores, arranged in a chevron configuration. The pores have a length-to-diameter ratio (L/D) of 60, making the thickness of each plate 1.2 mm. The plates are coated with a resistive layer by ALD with a target resistance of between 10 and 40 MΩ [9]. The plates are chosen within a pair to be matched in resistance within $\pm$10%.

To provide structural rigidity and the ability to support atmospheric pressure on the top and bottom of the package, the gaps in the vacuum volume from the cathode to the first MCP, from the first to the second MCP, and from the second MCP to the anode, are formed by spacers consisting of thin flat glass grids. The HV resistive divider chain is completed by coating the grid spacers with a resistive layer, also by ALD, as shown in Fig. 2.

The parameters of the layers that make up the tile are given in Table 1 [10]. A 2-mm grid spacer, shown in Fig. 4, sets the height and voltage across the photocathode–MCP gap and the gap between the two MCPs. A 6.5-mm grid spacer similarly sets the height and voltage across the gap between the bottom of the second MCP and the anode plane. The grid spacers are aligned to minimize the occluded area and to transfer the force of atmospheric pressure in columnar fashion between the top and bottom plates.

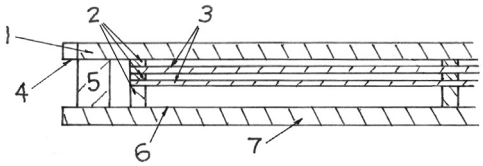

Fig. 1. The mechanical construction of the LAPPD™ module. All components are glass. The hermetic volume is formed by the top window (1), the side-wall (5), and the bottom plate (7). The photocathode is deposited on the inside of the window, and makes contact with the external HV input through a metalized border (4). The grid spacers (2) and the MCPs (3) are coated with ALD. The bottom plate (7) has silk-screened silver anode 50 Ω microstrips fired on its surface (6) that penetrate a frit seal under the sidewall and connect to the digitizing electronics.

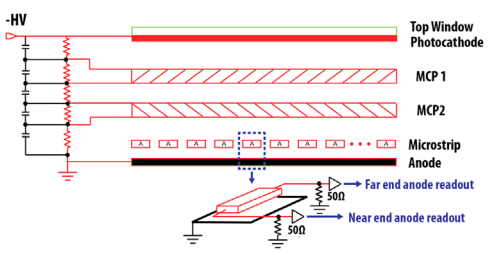

Fig. 2. The equivalent electrical circuit of the tile assembly. The upper diagram shows the DC circuit. The HV voltage divider is implemented by resistive ALD coatings of the grid spacers and the MCPs (see Fig. 1).

Table 1
A tabulation of the layers in the tile assembly, starting with the top window and ending with the bottom anode layer. Mechanical stability against atmospheric pressure is provided by a glass grid spacer in each of the three gaps, as listed. All components except the microchannel plates are made from B33 borosilicate glass plate [7].

Layer	Thickness (mm)	Material	Resistive coating	Metalization (side)
Window	2.75	B33	Photocathode (bottom)	Nichrome border (bottom)
Grid spacer 1	2.0	B33	ALD-GS	None
MCP 1	1.2	Micropore	ALD-MCP	Nichrome (both)
Grid spacer 2	2.0	B33	ALD-GS	None
MCP 2	1.2	Micropore	ALD-MCP	Nichrome (both)
Grid spacer 3	6.5	B33	ALD-GS	None
Anode	2.75	B33	N/A	Silver strips (top)

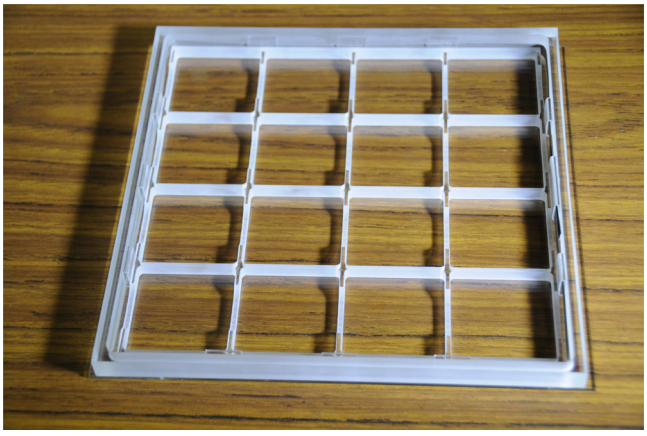

Fig. 3. A partial assembly showing the 'bottom' spacer grid, the getter strip and its supporting glass beads, and the sidewall as they would be in the assembled tile base. The 2.3 cm by 0.076 indentations that allow the separate vacuum volumes in the tile to communicate with each other are visible as channels running from left to right on the top edges of the spacer.

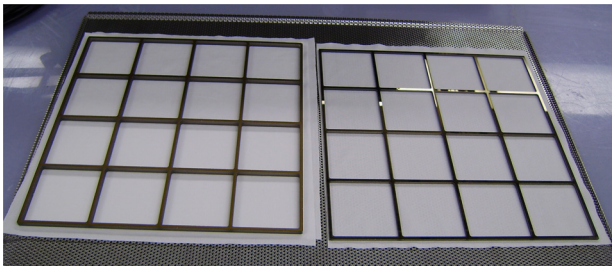

Fig. 4. Two of the glass grid spacers after the resistive ALD coating has been applied. The grid spacers are cut from easily available B33 glass [7]. Mechanically, the spacers serve to transmit the compressive force of atmospheric pressure from the top to the bottom of the tube; electrically the resistive coating provides the voltage drop across each gap. Metalization of the top surface of the top spacer can serve to provide distribution of HV across the (resistive) photocathode.

A 2.3 cm by 0.076 cm cut-away indentation in each crossbar in one direction in the bottom spacer allows the vacuum volumes defined by the spacer grid to communicate with each other for pumping, as shown in Fig. 3.

We have made tests with a Nichrome coating on the grid spacers and without. Because the MCPs are metalized with Nichrome top and bottom there is no need to metalize the grid spacers at those interfaces. However metalization of the top surface of the top spacer can provide a convenient method of distributing HV and current across the face of the (resistive) photocathode. The silver anode microstrips distribute the DC ground potential under the bottom spacer, which cannot be metalized without shorting the strips.

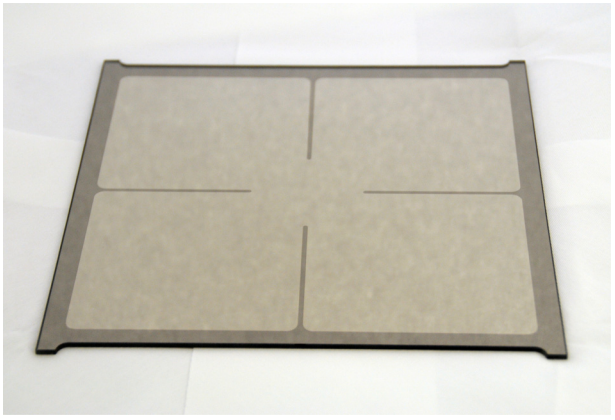

Fig. 5. The glass window showing the Nichrome border that is the 'tie layer' supporting the indium seal to the glass sidewall. The external tabs and the metalized border also supply the input HV to the cathode and resistive divider. The view is from the air-side (top); the Nichrome metalization for the seal and the HV distribution is visible on the vacuum-side (underneath) along the perimeter and on the four lands extending into the interior of the cathode.

2.2. DC current path

The DC electrical circuit of the photodetector is shown in Fig. 2. High voltage is applied to a Nichrome border on the underside of the window via a tab that extends beyond the sidewall. The Nichrome makes contact with the top grid spacer to supply current to the resistive divider through the spacers and MCPs.

Fig. 5 shows the window, including the external tabs and Nichrome border that supply the input HV to the photocathode and the divider. The HV is applied to the underside of two of the tabs, and connects to the cathode through the metalization for the seal. The four metalized lines that extend into the cathode provide HV distribution to the cathode plane, complementing the distribution from the top spacer.

The internal five layers, consisting of three grid spacers and two MCPs, form a resistive voltage divider [11] that passes a nominal 100 μA divider current from the cathode to the anode. Table 2 gives the nominal resistance and voltage drops across the divider.

The final step in the DC return path to HV ground is at each end of the anode microstrips, where individual 10 KΩ resistors terminate each strip to the copper substrate sheet that forms the signal ground-plane of the microstrips and the HV DC return, as shown in Fig. 2.

2.3. The signal path for fast-risetime pulses

The pulses from photons incident on the photocathode have sub-ns risetimes, with typical bandwidths for the present 20 μm-pores in the 1–2 GHz range. The DC HV path and the path of the fast signal pulses share the same HV distribution and

Table 2
The target resistances and nominal voltage drops in the internal HV divider. The divider current is set at 100 μA, corresponding to a limit of approximately 1 μA of current drawn from signal pulses [11].

Layer	Resistance (MΩ)	Voltage drop (v)
Grid spacer 1	2	200
MCP 1	10	1000
Grid spacer 2	2	200
MCP 2	10	1000
Grid spacer 3	6.5	650
Total	28.5	3050

ground. For the signal path, however, there are two configurations we have considered, a 'normal' one in which the charge of the fast signals is collected and recorded from the anode microstrips inside the vacuum volume, and an 'inside-out' geometry in which the anode is a thin metal layer that serves as a DC ground, but is thin enough so that the fast signal pulses capacitively couple through to strips or pads on the external side of the bottom plate. These are described in turn below.

2.3.1. Normal anode configuration

The signal path maintains the 50 Ω impedance of the strip onto the printed circuit card containing the waveform sampling 6-channel PSEC4 ASICs [12] that digitize the signals. The thickness of the anode glass plate and the width of the strips determine the impedance of the microstrip lines [4,13]. While the choice of impedance depends on a number of considerations, we chose a 50 Ω impedance for convenience in testing to match cabling and oscilloscope impedances. The choice of the anode plate thickness is application specific, with impedance, strip parameters, occupancy, weight, cost, amount of inactive material in the path of charged particles being some of the considerations. After the plate thickness is chosen the width of the anode strips can be set so to determine the characteristic impedance. A further parameter is the gap between strips, which is vulnerable to charging in high-rate applications if electric field lines terminate on the dielectric.

Each 50 Ω stripline is impedance-matched to the PC cards that digitize the signals and that mate with the edge of the end tiles of a tile row, as shown in Fig. 6. The DC return for the divider current through the 10 KΩ resistor has a much higher impedance than the 50 Ω signal path. For flexibility in testing, an easily removable connection was made using low profile electro-magnetic interference (EMI) shielding gaskets [14]. Each EMI gasket strip was cut at the pitch interval into separate RF fingers and mounted on a 1/2 in. G10 bar to match the anode spacing. Fig. 6 shows the connections between the strips on the tile and the strips on the PC card used for testing the tiles.

2.3.2. The 'inside-out' anode

There are a number of applications, such as large collider detectors in HEP and some medical imaging cameras, that would have many particles arriving in a narrow time window and consequently high occupancies in a strip-line readout. These applications would benefit from a 2-dimensional 'pad' readout rather than a 1-dimensional stripline geometry.

The fast risetime of the signal pulses from the MCP amplification chain provides a mechanism to extract the signals from the vacuum volume by capacitively coupling through the glass anode bottom plane. In this 'inside-out' implementation, a uniform metal layer thinner than a skin-depth at frequencies characteristic of the MCP risetime is deposited on the inner (vacuum-side) side of the anode bottom glass plate, replacing the microstrips. This layer provides the ground return for the DC HV current. The outer (air-side) side of the anode plate supports the readout pattern deposited by metalization, typically in pads or strips. This layer can then be connected to the electronics and additional grounds as necessary.

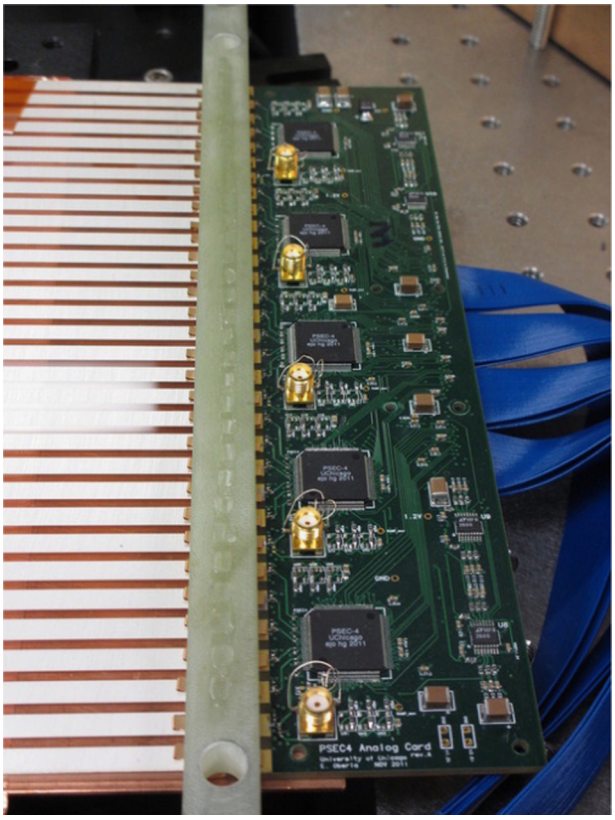

Fig. 6. A picture showing the interface between the tile anodes and the readout system at the end of a row of tiles. The DC path to HV ground at the end of the microstrips is through individual 10 KΩ resistors on each strip to HV ground on the analog card that holds the waveform sampling ASICs. To allow easy disconnection for testing, a bar of FR4 with RF-fingers is used to bridge the gap between each of the 30 strips on the tile to the corresponding strip on the PC card.

3. Implementation in the LAPPD™ package

The LAPPD™ design integrates the mechanical structure with both the high frequency signal path and the HV DC current path into a single economical structure. The advantage of the integrated design is that the construction is planar, with all electrical connections lying in the same plane as the thin form-factor detector module itself. This allows a 'tiling' of large areas with a higher filling factor than would be possible with individual modules with edge-readout. We give details of the implementation below.

3.1. Mechanical dimensions

The tile assembly is a flat glass package with transverse dimensions of 229.1 mm in the strip direction by 220 mm transverse. The active area is 203 mm by 203 mm (8 in. by 8 in.). The current prototype grid spacers occlude 16% of the active area; this will be reduced in future designs after more experience with this first-generation simple implementation.

A mockup of an assembled glass module, made with prototype glass parts but without a photocathode or vacuum seal, is shown in Fig. 7. Multiple modules can be integrated into a 'supermodule', sharing the RF-strip-line readout mounted on the 'tray' that also supports the electronics, as shown in Fig. 8 [4].

The tile is made from glass layers stacked to form a rigid structure when compressed by atmospheric pressure. The vacuum

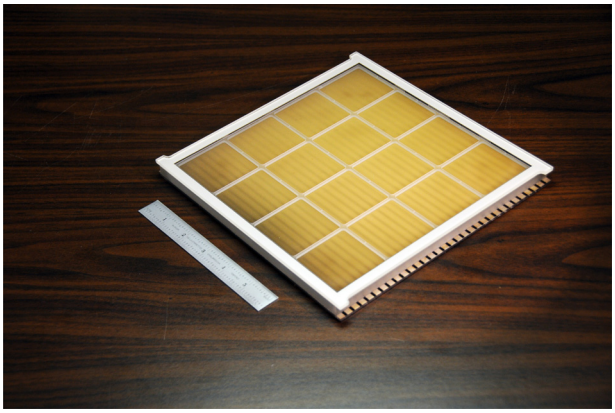

Fig. 7. An 8 in.-square (20 cm-by-20 cm) LAPPD™ module ('tile'). The tiles are hermetically sealed vacuum tubes that provide the photocathode and MCP-based amplification chain. The upper layer of the micro-strip RF transmission lines that form the anode are on the internal surface of the bottom plate of the tile; the ground plane of the transmission line is the upper surface of the supporting 'tray', shown in Fig. 8. The thin format and modular nature of the photodetector allow application-specific optimization.

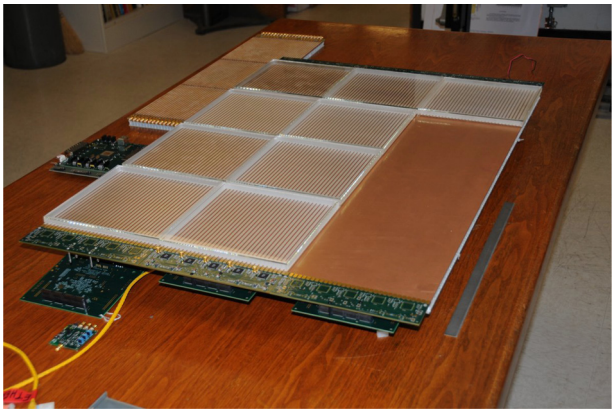

Fig. 8. A 'supermodule' consisting of twelve 8 in.-square LAPPD™ modules ('tiles') mounted on a 'tray' that provides the ground plane for the anode micro-strips and the support for the digitizing electronics at each end. Each row of four tiles shares the same anode strips in series, as described in Ref. [4].

volume is enclosed by the 2.75 mm-thick top window, a standard plate glass thickness. The photocathode is on the bottom surface of the window, facing the top of the upper MCP (see Fig. 1). The anode plate with silver microstrips on its top surface, serves as the bottom of the vacuum volume, and is also 2.75 mm-thick. A rectangular border of 5.08 mm (0.200 in.) width, cut from a standard thickness glass plate, forms the sidewall of the volume.

The sidewall is sealed to the anode plate over the microstrips with a glass frit seal. The metal microstrips extend beyond the sidewall so that contact can be made with neighboring tiles [4] or the digitization printed circuit cards at the end of a tile-row [12].

4. Performance of the HV divider

The proposal to use ALD coatings on the grid spacers and MCPs to determine the amplification and transport voltages had unknown risks at the outset of the LAPPD program. In particular we are relying on the stability of the coatings under a large mechanical pressure. Atmospheric pressure corresponds to almost 1200 lbs on the top and bottom plates. The pressure on the MCP surfaces is magnified by the ratio of areas of the grid spacer to the total area, approximately a factor of 10. The surfaces of the MCPs consist of glass capillaries with ~65% open area, and have both metal electrode material and ALD secondary-emitting material; the surfaces of the grid spacers have a grid-specific ALD resistive coating. How these interfaces behave under pressure, with temperature, and over time is not tractable to calculation; we have consequently embarked on a series of measurements of the stability of the HV divider assembly under HV and pressure. Several of the test facilities are described in turn below.

4.1. Test facilities

Section 4.1.1 describes a custom test facility, the spacer station (ISS) used to make DC measurements of current and voltage. A second test facility, the 'demountable tile', consisting of an actively pumped glass-body tile mechanical assembly with an O-ring top seal, is used to make measurements of fast pulses at resolutions down to 5 ps, as described in Section 4.1.2.

4.1.1. The spacer station (ISS)

To measure the resistance of the grid spacers and MCP plates vs. pressure, temperature, and over time, a simple flat square vacuum vessel with a flexible lid consisting of an aluminum foil incapable of withstanding atmospheric pressure was constructed. The window provides the same (atmospheric) pressure on the component stack as the glass window of the sealed tile. Fig. 9 shows the ISS open to air with a single grid spacer inside. The copper plate to the right of the ISS provides HV contact to the layers being measured; the ISS frame is the DC ground. Single, multiple, or a full stack of the component layers (grid spacer and MCP) can be measured using suitable non-conducting spacers above the copper plate.

4.1.2. The demountable tile

In order to test the time and position response of the photodetectors as a system we have constructed a facility [15] of which the key components are a pulsed Ti:Sapphire laser with a pulse width ~100 fs, and a data-acquisition system with 60 channels of 10–15 GS/s waveform sampling readout, shown in Fig. 10. The demountable tile is constructed with the anode frit-sealed to the sidewall and the internal HV divider as in the LAPPD™, but has a removable window sealed with an O-ring so that MCP plates can be

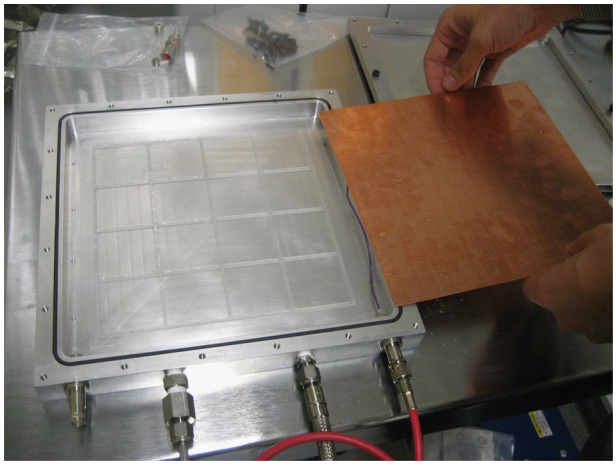

Fig. 9. The spacer station (ISS) used to measure resistances of individual grid spacers, MCPs, and the complete divider. A grid spacer is shown in the vacuum volume; the copper plate being held on the right is an electrode that supplies the HV to the piece being measured. A thin insulating layer separates the copper HV electrode from the 2.75-mm-thick top window, which is thin enough that atmospheric pressure deflects it until stopped by the internal stack of MCPs and grid spacers, compressing the divider.

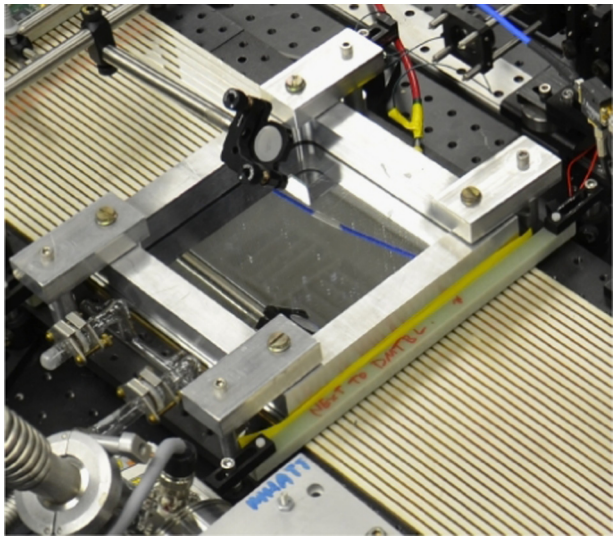

Fig. 10. The demountable tile test setup, consisting of glass tile of the LAPPD™ design constructed with the LAPPD™ hermetic package and internal divider, but with a removable window sealed with an O-ring. The tile consequently has to be actively pumped, and, as a bialkali anode cannot survive in air, has an aluminum cathode. However the HV divider and signal circuit are the same as in the sealed tile. The tile is shown sitting on a 4-tile anode readout 'tray', which is equipped with 60 channels (30 strips on each end) of 10–15 GS/s waveform sampling PSEC-4 ASICs.

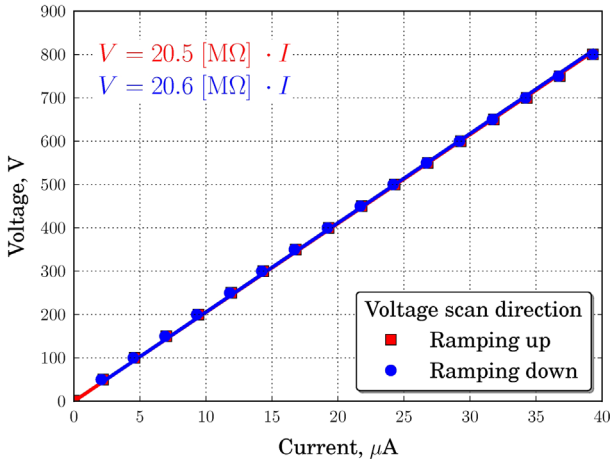

Fig. 11. The current-vs.-voltage (I–V) data for the ALD-based HV divider, as measured in the ISS test facility. The voltage is measured both ramping up and ramping down increased (red, squares) vs. decreased (blue, circles). The slope gives the effective resistance of the multi-layer divider. (For interpretation of the references to color in this figure caption, the reader is referred to the web version of this paper.)

easily inserted and removed for rapid testing. The tile consequently has to be actively pumped, and has an air-stable aluminum cathode.

The HV control system for the demountable tile test facility allows for measuring voltage and current under computer control [15], and similarly measuring the stability of the gain and spatial response over the face of the tile [16].

4.2. Current-vs.-voltage (I–V) curves

One concern about using ALD-coated elements as a HV divider is the possible non-linear or non-reproducible behavior as a function of voltage. Fig. 11 shows the measured I–V curve using the ISS facility. The behavior is linear, and demonstrates little hysteresis.

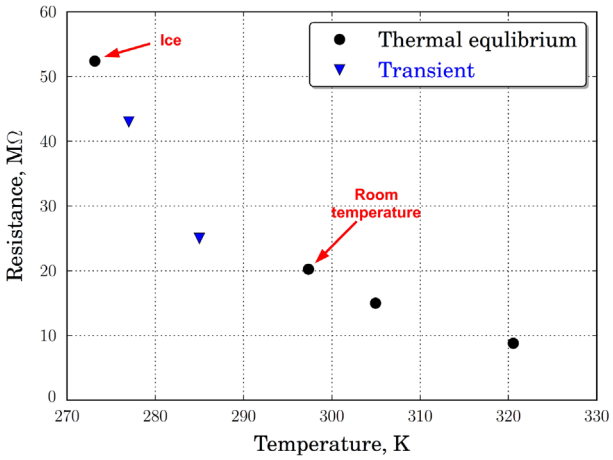

Fig. 12. The resistance of the HV divider as a function of temperature. The measurements between room temperature and the temperature of ice were measured by necessity 'on the fly', rather than in thermal equilibrium, a possible explanation of the apparent offset from the curve.

4.3. Thermal coefficient

The temperature dependence of the divider resistance is of concern due to the vulnerability of MCP-based photodetectors to thermal run-away [17]. The divider resistance depends on the thermal coefficients of the ALD-coatings of the grid-spacers and MCPs. The resistivity of the coatings on the grid spacers is different from that for the MCPs, as the effective conducting areas are so different. At present the three grid spacers are coated in the same batch, so the difference in resistance is determined solely by the difference in the conduction path length of the thicker grid spacer from that of the other two (see Table 1). Fig. 12 shows the resistance of the HV divider as a function of temperature, measured in the ISS.

4.4. Pressure dependence

The contacts between the grid spacers and the MCPs are complex electrically and mechanically [18]. The spacer station (ISS) was constructed with a thin foil top 'window' specifically to measure the contact resistances vs. pressure. The pressure is varied by control of the vacuum inside the ISS through a needle valve to the pump. A curve of resistance vs. the pressure on the layers of the HV divider (lbs/in.^{2}) is shown in Fig. 13. The drop in resistance of approximately 20% at low pressure is presumably due to changes in contact. A small amount of hysteresis is observed; however in an operating evacuated tile the pressure on the stack is stable, with only minor variations due to changes in atmospheric pressure or temperature.

4.5. Long-term stability

The large pressure (>1000 lbs) on the HV divider transmitted through the thin glass top window and bottom plate is also a cause for concern about the long-term stability of the electrical contacts between the layers that constitute the divider. The mechanical and electrical stability of the interface are subject to changes due to pressure, electro-chemistry, and temperature, as well as a possible slow creep of a component or layer under the pressure. Over the course of 11 months under vacuum, a stack of two MCPs and 3 grid spacers the demountable tile has remained stable in resistance, gain, and uniformity, giving us confidence in the mechanical design.

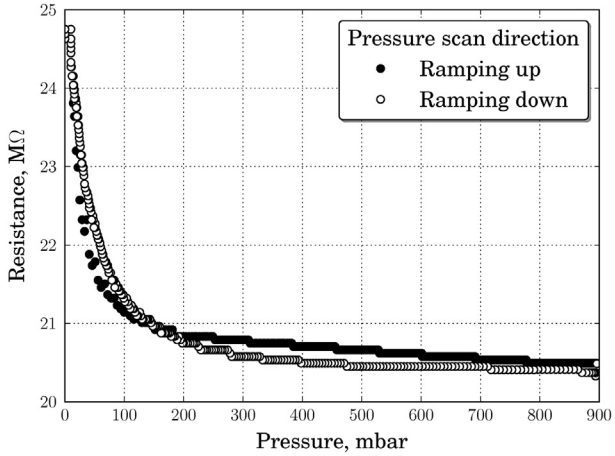

Fig. 13. The resistance of the HV divider as a function of the pressure compressing the divider stack. The pressure is varied by using the differential between atmospheric pressure on one side of the thin foil window at the top of the ISS and the partial vacuum inside the volume. The pressure in the ISS is controlled by pumping through a needle valve. Note the suppressed zero on the ordinate.

5. Conclusions

The use of ALD for functionalizing glass capillaries and glass grid spacers enables a modular compact design of a thin planar photodetector with an internal HV divider. The LAPPD^{TM} module is simple, consisting of eight parts, all made of glass, and a simple getter assembly. The amplification section consists of two 203 mm-by-203 mm MCPs. The HV divider is formed by applying resistive coatings to the grid spacer in each of the three gaps: between the photocathode and MCP1, between MCP1 and MCP2, and between MCP2 and the anode microstrip transmission lines.

The sealed module sits flat on a ground plane that is shared with neighboring modules; there are no connecting pins on the back side. The HV is applied to an external metalized tab that connects to the metal top seal between the window and the glass sidewall. The DC ground is provided by the anode ground plane of microstrips, which are deposited on the top surface of the glass bottom plate of the hermetic package, and extend through the seal to outside the vacuum volume. The anode microstrips can be connected in series to form a continuous anode up to 90 cm long, with the DC ground return and ASIC readout on the ends of the outer-most modules [4].

Measurements of current vs. voltage in the HV divider have been made in a custom test setup and in the module glass body on a 90-cm anode. The measurements in the test setup have been made as a function of the pressure on the divider, controlled by varying the vacuum in the module. Measurements of the temperature dependence and stability are also presented. An 11-month test under vacuum gives us confidence in the long-term stability of this relatively simple integrated electro-mechanical design.

Acknowledgments

We thank our colleagues in the Large Area Picosecond Photodetector (LAPPD) Collaboration for their contributions and support. Special thanks are due to A. O'Mahony (Incom) and Neal Sullivan (Arradiance) for their essential work on ALD coatings for the components of the internal stack. Thanks are due to R.G. Wagner (ANL) for technical support; D. Walters and J. Williams (ANL) for metalization of the windows and vacuum expertise; and H. Wen and H. Gibson (ANL) for laser and electronics support at the APS testing lab. We are deeply grateful to E. Hahn (Fermilab) for meticulous metalization of the MCPs, and P. Murat (Fermilab) for support. R. Metz (UC) provided expert machining of test setups and glass parts. M. Heintz (UC) supplied crucial technical and computer systems support. We thank Q. Guo (UC), Chian Liu (ANL) and H. Clausing (H. Clausing, Inc) for expert advice and large amounts of time teaching us about cleaning and metalization of glass. We also thank our superb glass vendors P. Jaynes (CatI Glass, Inc) and P. Seegebrecht (Webcorr) for metalization and glass. The activities at Argonne National Laboratory were supported by the U.S. Department of Energy, Office of Science, Office of Basic Energy Sciences and Office of High Energy Physics under contract DE-AC02-06CH11357, and at the University of Chicago by the Department of Energy under DE-SC-0008172, the National Science Foundation under Grant PHY-1066014, and the Driskill Foundation.

References

[1] The original LAPPD institutions include ANL, Arradiance Inc., the University of Chicago, Fermilab, the University of Hawaii, Muons, Inc, SLAC, SSL/UCB, and Synkera Corporation. More details can be found at ⟨http://psec.uchicago.edu/⟩.
[2] J.L. Wiza, Nuclear Instruments and Methods in Physics Research 162 (1979) 567.
[3] E. Oberla, Ph.D. thesis, in preparation. We thank H. Nicholson for the original suggestion of using large-area planar detectors for water Cherenkov neutrino detectors, and for the OTPC name.
[4] H. Grabas, R. Obaid, E. Oberla, H. Frisch, J.-F. Genat, R. Northrop, F. Tang, D. McGinnis, B. Adams, M. Wetstein, Nuclear Instruments and Methods in Physics Research Section A 71 (2013) 124.
[5] The glass capillary substrates are produced by Incom Inc. Charlton Mass. See ⟨http://www.incomusa.com/⟩.
[6] S.M. George, Chemical Reviews 110 (1) (2010) 111;
J.W. Elam, D. Routkevitch, S.M. George, Journal of the Electrochemical Society 150 (6) (2003) G339;
D.R. Beaulieu, D. Gorelikov, H. Klotzsch, P. de Rouffignac, K. Saadatmand, K. Stenton, N. Sullivan, A.S. Tremsin, Nuclear Instruments and Methods in Physics Research Section A 633 (2011) S59;
O.H.W. Siegmund, J.B. McPhate, S.R. Jelinsky, J.V. Vallerga, A.S. Tremsin, R. Hemphill, H.J. Frisch, R.G. Wagner, J. Elam, A. Mane, Development of Large Area Photon Counting Detectors Optimized for Cherenkov Light Imaging with High Temporal and Sub-mm Spatial Resolution, NSS/MIC 2011 IEEE, October 2011, p. 2063.
[7] ⟨http://psec.uchicago.edu/glass/borofloat_33_e.pdf#page=28⟩. The dielectric constant is 4.6 and the loss tangent is 37×10^{-4}, both measured at 25 °C and 1 MHz.
[8] Ferro Corp., 251 Wylie Ave., Washington PA 15301. We are grateful to E. Axtel for extensive assistance with selecting the silver ink for silk-screening the anode microstrips.
[9] A.U. Mane, W.M. Tong, A.D. Brodie, M.A. McCord, J.W. Elam, ECS Transactions 64 (9) (2014) 3;
A.U. Mane, J.W. Elam, Chemical Vapor Deposition 19 (2013) 186.
[10] The tabulated values are those in current use. They can be changed to optimize the voltages across the respective gaps for specific performance goals. The total thickness depends on the height of the sidewall, which also can be optimized for different applications.
[11] S.-O. Flyckt, C. Marmonier, Photomultiplier Tubes: Principles and Applications, Photonis Brive, France, 2002.
[12] E. Oberla, H. Grabas, J.F. Genat, H. Frisch, K. Nishimura, G.S. Varner, Nuclear Instruments and Methods in Physics Research Section A 735 (2014) 452.
[13] For an excellent discussion of transmission lines, see E. Bogatin, Signal Integrity Simplified, Prentice Hall Professional Technical Reference, 2004. Chapter 10 is especially clear on cross-talk in striplines.
[14] Leader Tech part number 12-60LPAH-BD-16 Laird Technologies, Item 97-115.
[15] B. Adams, M. Chollet, A. Elagin, R. Obaid, E. Oberla, A. Vostrikov, P. Webster, M. Wetstein, Review of Scientific Instruments 84 (2013) 061301.
[16] B. Adams, A. Elagin, M. Wetstein, et al., Nuclear Instruments and Methods in Physics Research Section A 732 (2013).
[17] C.W. Carlson, J.P. McFadden, Design and application of imaging plasma instruments, in: R.F. Pfaff, J.E. Borovsky, D.T. Young (Eds.), Measurement Techniques in Space Plasmas: Particles, American Geophysical Union Publications, Washington DC, USA, 1998.
[18] The measurements presented here are made with MCP's that have the electrode surface 'under' the ALD resistive and emissive coatings. The other option, 'over', has the electrode on top of the ALD coatings. Both options have their merits and drawbacks.